Ann. Rev. Mater. Sci. 1977. 7:73–93

TRANSPARENT CONDUCTING COATINGS

G. Haacke
American Cyanamid Company, Stamford, Connecticut 06904

INTRODUCTION

The simultaneous occurrence of electrical conduction and optical transparency in thin solid films has been utilized since the last century. It appears that thin film electrodes of silver (1) and platinum (2) on selenium photoelectric cells were the first reported applications of transparent conductive coatings. Transparent metal electrodes in the form of thin gold leaves were used even earlier, specifically as front electrodes in photoconductive and photovoltaic selenium cells (3).

Commercial usage of transparent electrically conductive coatings became a reality during the 1930s when the first solid-state photodetectors appeared on the market. These early devices were either copper oxide (4) or selenium (5) Schottky barrier cells with transparent metal front electrodes. The metal films consisted mainly of extremely thin sputter-coated gold or silver (6), and sometimes copper layers (7).

Practical application of transparent conducting coatings increased significantly after the introduction of wide-band-gap semiconductor films. Tin oxide coatings (8) were utilized during the last war and developed swiftly into commercial products (e.g. Nesa glass) since they could be easily manufactured by spray deposition. Indium oxide layers existed as early as 1950 (9), but did not become commercially available until recently (10).

The high transparency of the oxide conductors combined with mechanical hardness and good environmental stability have opened up numerous applications for the conductors, including heating elements on aircraft windows for de-icing and defogging, antistatic coatings on instrument panels, electrodes in electroluminescent lamps and displays, electrodes in imaging devices, and ferroelectric memories. The development of modern liquid-crystal (11) and electrochromic (12) displays would have hardly been possible without transparent oxide electrodes.

Renewed worldwide interest in solar energy conversion may enhance the applications potential of transparent conductors far beyond its present limits. The incorporation of transparent oxide electrodes into solar cells has been proposed and is under development (13–15). For this application, the electrical and optical properties of the coatings need to be improved significantly over current commercial

products. In competition with tin and indium oxide, a third oxide, cadmium orthostannate (Cd_2SnO_4), is now under development and shows considerable promise as a high-transparency, high-conductivity material (16).

The large free-carrier concentrations attainable in high conductivity oxides shift the plasma-reflection edge to near-infrared wavelengths and induce high reflectivities beyond the plasma edge. This property, in combination with high transparency to solar radiation, can be exploited for heat-reflective coatings in solar thermal collectors (17, 18). Although this particular application of transparent conductors could assume great practical importance, it is not discussed further in this review.

Many semiconducting compounds transmit light as thin films, and therefore could qualify for transparent electrode coatings. For reasons explained in the next section, this paper includes only materials which are known to reach electrical conductivities of at least 1000 ohm^{-1} cm^{-1} and still maintain good optical transparency. Besides semiconductor coatings, thin metal films are reviewed since certain applications require the unique properties of these materials.

MATERIALS EVALUATION

The usefulness of a transparent conductor is determined primarily by its optical transmission and electrical conductivity. Both parameters should be maximized. Additional properties important to practical applications are environmental stability, abrasion resistance, and compatibility with the substrate and other components of a given device. Raw materials availability and economics of deposition become decisive factors when large-scale utilization is considered. In this section, a general analysis of the fundamental electrical and optical materials properties is presented and criteria established which may assist in developing new coatings. Other parameters, mentioned above, are discussed for individual conductors in subsequent sections.

Transparent electrodes can be readily evaluated by calculating the figure of merit (19)

$$\phi_{TC} = T^{10}/R_s \qquad 1.$$

where T is the optical transmission and R_s is the electrical sheet resistance. The parameters T and R_s can be measured without difficulty so that the determination of ϕ_{TC} is a matter of routine.

For an analysis of ϕ_{TC} we note that

$$T = \exp(-\alpha t) \qquad 2.$$

and

$$R_s = 1/\sigma t, \qquad 3.$$

where α is the optical absorption coefficient in cm^{-1}, σ is the electrical conductivity in ohm^{-1} cm^{-1}, and t is the film thickness in cm. The dimension of the sheet resistance is given in "ohm per square" to indicate that it measures the resistance of a film with square surface area.

Equation 3 points to the need for high electrical conductivities to achieve low sheet resistances unless t is made unreasonably big. For instance, if $R_s = 10$ ohm/sq is specified a coating thickness of 10^{-4} cm will be required when $\sigma = 10^3$ ohm^{-1} cm^{-1}. With the same conductivity we would need $t = 10^{-3}$ cm to reach $R_s = 1$ ohm/sq. Such a coating is not only difficult to prepare but, in most cases, also absorbs too much light. Electrical conductivities larger than 10^3 ohm^{-1} cm^{-1} are therefore required for a good transparent conductor and, in view of a growing demand for coatings in the 1 ohm/sq range, conductivities approaching 10^4 ohm^{-1} cm^{-1} will become essential.

Equations 1, 2, and 3 can be combined to

$$\phi_{TC} = \sigma t \exp(-10\alpha t). \qquad 4.$$

Knowledge of the materials parameters α and σ allows us to calculate ϕ_{TC} as a function of t for any material and determine its maximum value. Figure 1 shows

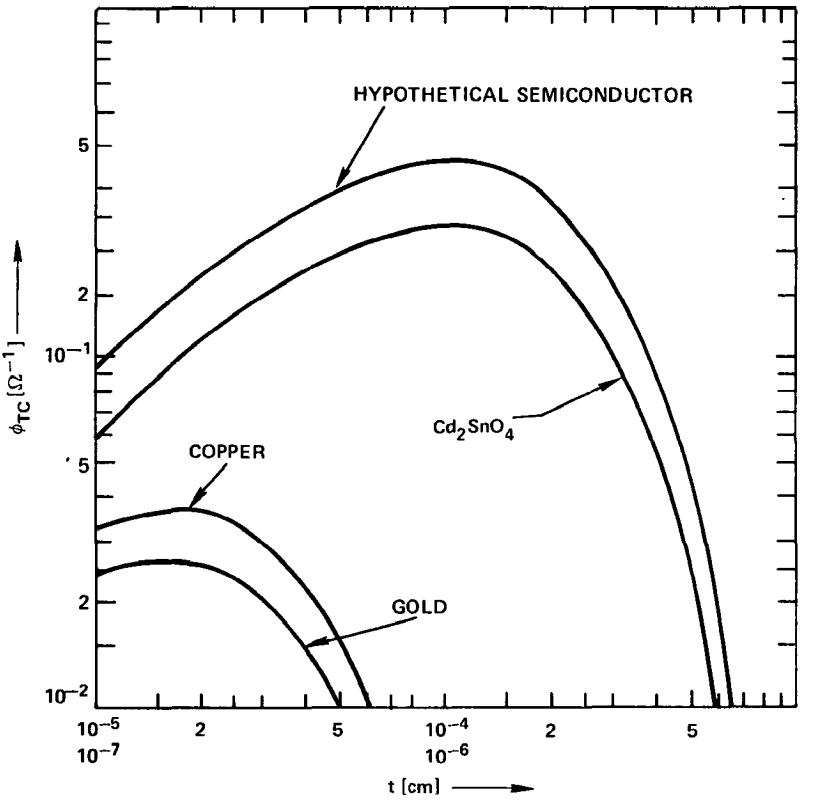

Figure 1 Calculated figure of merit ϕ_{TC} versus film thickness at 5500 Å wavelength for metal and semiconductor films; upper abscissa for semiconductors, lower abscissa for metals.

examples of two metals and two semiconductors with the α-values chosen at 5500 Å wavelength. The metal curves were calculated from the bulk values of α and σ, while for Cd_2SnO_4 actual thin film data ($\sigma = 6 \cdot 5 \cdot 10^3$ ohm^{-1} cm^{-1}, $\alpha = 10^3$ cm^{-1}) were available. The hypothetical semiconductor was assumed to have $\sigma = 10^4$ ohm^{-1} cm^{-1}, $\alpha = 10^3$ cm^{-1}; these values appear to be feasible in materials such as Cd_2SnO_4 or In_2O_3.

Figure 1 demonstrates that the highest figures of merit occur in semiconductors. Moreover, we see later that the metal curves represent upper limits for this class of materials, while it is reasonable to expect that further improvements will be achieved in transparent semiconductor coatings.

The preceding analysis can be extended to more fundamental considerations. Assuming a given sheet resistance, equation 4 leads to

$$\phi_{TC} \sim \exp\left(-\text{const}\frac{\alpha}{\sigma}\right)$$

This relation shows that α/σ is the basic materials parameter determining the figure of merit of a transparent conductor. For reasons of convenience, the dependence of ϕ_{TC} on σ/α rather than on α/σ is discussed below.

The electrical conductivity is related to α by

$$\sigma/\alpha = \pi c n v^2 \tau^2 \qquad 5.$$

if free-carrier absorption is the principal absorption mechanism (20). Here c is the velocity of light, n is the index of refraction, v is the light frequency, and τ is the free-carrier relaxation time. Equation 5 is based on classical electron theory, but this relation also holds remarkably well for degenerate semiconductors and metals (21).

The relaxation time in equation 5 can be replaced by the carrier mean free path l, according to $\tau = l/v$, and then we see that the highest figures of merit should be found in materials with large mean free paths. For metals the mean free path is of the order of 10^{-6} cm (22), while for semiconductors it is of the same order of magnitude or higher (23). The high absorption of metals in the spectrum's visible region requires very thin films ($\sim 10^{-6}$ cm) to achieve sufficient transparency. At such thicknesses diffuse scattering of the charge carriers at the film surface considerably reduces the mean free path (24). Furthermore, agglomeration effects add another important component to increased resistivities in thin metal films. These effects are negligible in transparent semiconductor layers since their low optical absorption permits t values beyond the surface scattering and agglomeration ranges.

Equation 5 can be converted into a form more suitable to semiconductors by substituting the carrier mobility μ for τ according to $\mu = e\tau/m^*$ where e is the electron charge and m^* the effective mass. The introduction of μ yields

$$\sigma/\alpha = \frac{\pi c n v^2}{e} \mu^2 m^{*2}. \qquad 6.$$

In semiconductors the relation $\mu \sim (m^*)^{-x}$ holds, and it has been shown that for many materials $x = 1.35$ (25). Equation 6 now allows us to formulate the following rule: good transparent conductor properties should occur in semiconductors with high mobilities or a low effective mass.

METAL FILMS

The analysis in the preceding section led to the conclusion that semiconductors yield better transparent conducting coatings than metals when judged by the figure of merit. The utility of a coating, however, is not solely determined by ϕ_{TC}. In many cases other characteristics are of equal or greater importance. The particular properties which assure metals practical utilization include chemical compatibility, work function, and fast deposition by evaporation. A major disadvantage of thin metal films is their lack of hardness so that protective coatings or laminates are often needed for protection.

Two principal difficulties impede the realization of the theoretical figure of merit in transparent metal electrodes. First, the nucleation and growth mechanism of metal films leads initially to the formation of island structures (26), which increase the sheet resistance far above the values expected from the bulk conductivity. After attainment of film continuity, diffuse electron scattering at the film surface reduces l until the film thickness exceeds the mean free path of the bulk material (27). Second, metal films are opaque. A detailed discussion of these effects is beyond the scope of this review and can be found elsewhere (28).

High optical reflectance losses are also frequently cited against metal films. However, in the thickness range covering transparent metal electrodes (30–150 Å), the reflectivity decreases with t (29), and quite often becomes comparable to the reflectances found in semiconductors.

Despite the extensive research devoted to thin metal films, only transparent gold electrodes are currently used on a large scale. Applications include de-icing and defogging of automobile and aircraft windows, RFI/EMI shielding of aircraft canopies, and antistatic coatings. A future application with considerable potential could be the use of thin gold films in Schottky barrier solar cells (30). The gold film in this device is primarily employed to form the Schottky barrier, and its sheet resistance is quite high (~ 50 ohm/sq). To achieve maximum conversion efficiency, an auxiliary transparent electrode in the form of a grid contact or a continuous semiconductor oxide film is indispensable.

Thin gold films vacuum deposited onto glass substrates suffer from the adverse effects mentioned above. Their sheet resistance is higher than expected for the given transmissions. An example is included in Figure 2. Curve A was measured on gold films evaporated onto ultrasonically cleaned microscope slides using standard precautions of modern vacuum technology. The effects of surface scattering, island formation, etc, are clearly seen in the high-resistance region (small t) where the transmission fails to increase.

Acceptable transparent electrode properties can be obtained in gold films by

adding processing steps. Film continuity and surface smoothness improve when auxiliary thin film layers, such as ultrathin metal films (e.g. chromium) and/or transparent oxide layers are applied. The composition of these interlayers in commercial products is usually considered proprietary. Nevertheless, a few helpful hints have found their way into the open literature. Bismuth oxide is an effective interlayer material (31). In fact, optical transmissions as high as 82% and 4 ohm/sq sheet resistance were reported (32) in gold films sandwiched between two bismuth oxide films with optimized thickness (Figure 2, point *B*). Obviously, these multilayer film systems are economically less attractive than single-layer coatings and, in the case of bismuth oxide, may have unacceptable stability problems. Besides bismuth oxide, other useful interlayer materials for gold electrodes are the oxides of indium, lead, and antimony (33). Figure 2 (curve *C*) shows examples of commercially available gold films in which surface-scattering effects, etc, are reduced by proprietary processing and multilayer composition.

Oxide interlayers will not be acceptable in devices requiring good electrical contact between the gold electrode and the substrate. In these situations improved gold transmission can be achieved with zinc sulfide anti-reflective layers (34).

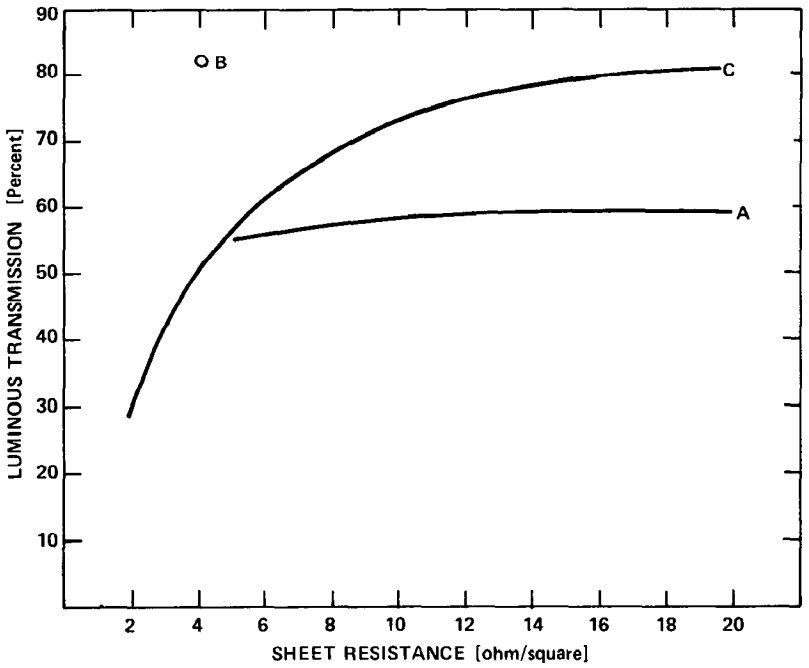

Figure 2 Luminous transmission versus electrical sheet resistance for transparent gold coatings. *Curve A:* evaporated gold films on microscope slides; *Point B:* reference 32; *Curve C:* commercial gold coatings on plastic substrates.

Electrical and optical bulk properties suitable for transparent electrodes also exist in silver and copper. Films prepared from these metals show aging effects when exposed to the atmosphere (26, 35), and thus are of limited practical utility. Chromium has been used in Schottky barrier solar cells, where it performs the dual function of barrier metal and transparent electrode (36). Alloying chromium with gold (36) or copper (37) results in better electrode performance. The alloying of metal films can also increase their corrosion resistance and improve adhesion, hardness, and weatherability (38).

Thin films of many noble metals have been investigated. Most of these materials are more difficult to evaporate than gold (39), and transparent electrode properties superior to those of gold may be hard to realize. Advantages over gold could be gained by better mechanical characteristics. For instance, rhodium films with good abrasion resistance can be prepared under suitable deposition conditions so that economic benefits could be derived from saving additional protective coatings (40). The transparent electrode properties of these films have not been reported.

SEMICONDUCTOR COATINGS

We have stated that materials with high carrier mobilities and a low effective mass should be good transparent conductors. The mathematical expressions supporting this reasoning are based upon absorption processes caused by free carriers only. This assumption implies that the useful transmission region of semiconductors is restricted to wavelengths longer than the band-gap energy. Since many applications require transmission over the entire visible spectrum semiconductors with band gaps close to 3 eV or larger are best suited.

The band-gap requirement places a severe restriction on the otherwise large number of semiconductors possessing attractive electrical transport properties. For example, indium antimonide because of its very low effective mass (0.013) and high electron mobility (78,000 $cm^2\ V^{-1}\ sec^{-1}$) should be an outstanding transparent conductor. Assuming that the bulk properties of InSb could be duplicated in thin films, sheet resistance and transmission can be estimated from published optical (41) and electrical (42) data. Indeed, a $2 \cdot 10^{-4}$ cm thick, antireflection-coated film would have 0.5 ohm/sq sheet resistance and approximately 95% transmission if doped with $10^{19}\ cm^{-3}$ donors (7000 $cm^2\ V^{-1}\ sec^{-1}$ mobility). Yet the utility of such a film is restricted to the 2.5–3.5 μm wavelength region because of the small InSb band gap (0.17 eV). The quoted transmission window is shifted by the Burstein effect to shorter wavelengths than would be calculated from the band gap.

Realization of bulk properties in InSb or any other semiconductor film is not easy. As in metal films, the electrical conductivities are usually lower than in bulk material. The mechanisms causing lower conductivities are different for the two classes of materials. The high optical transmission below the band gap permits ten to hundred fold thicker semiconductor electrodes than is possible with metals. Hence, size effects reducing the carrier mean free path are negligible. The same is true for growth effects such as island formation or agglomeration.

The important effects retarding the conductivity of semiconductor films arise at

least in part from their polycrystallinity. Single-crystalline transparent electrodes are not considered here since their large-area fabrication faces serious economic obstacles at the present state of technology. In a polycrystalline film, high- or low-angle grain boundaries scatter carriers and may also be responsible for the formation of potential barriers (43). In addition, dislocations as well as point defects, ionized impurities, and stress effects are known to reduce the carrier mobility. Later, it is shown that secondary phases can mask the transparent electrode properties of a semiconductor film appreciably. Structure and morphology also affect conduction and transmission of thin films. In general, amorphous transparent electrodes are inferior to polycrystalline coatings.

The negative influence of many effects mentioned above can be reduced if not eliminated, by carefully developed deposition techniques. A considerable amount of work has already been invested in some of the leading transparent semiconductors, and further improvements may be more difficult to achieve. Others have received limited attention thus far and could acquire desirable transparent electrode features if optimized preparation conditions can be established.

There are three semiconducting oxides known to possess transparent electrode properties of practical significance—tin oxide, indium oxide, and cadmium stannate. They are reviewed in the following sections, along with cadmium oxide which, because of its fundamental semiconductor characteristics, represents in many respects a model of a transparent conductor.

Cadmium Oxide

The electrical and optical properties of cadmium oxide, CdO, were explored in some detail in thin films (44–49) and sintered samples (50). Later work on single crystals confirmed the earlier results (51, 52). The general picture following from these investigations shows that CdO is an *n*-type semiconductor in which interstitial cadmium provides free electrons. Electron concentrations between $5 \cdot 10^{16}$ cm^{-3} and 10^{21} cm^{-3} have been obtained.

The outstanding feature of CdO is a large shift of the fundamental optical absorption edge from 2.3 eV to 2.7 eV when the free-carrier concentration increases. It is interesting to note that this shift was discovered in CdO (46) almost simultaneously with Burstein's interpretation (53) of the same effect in InSb. One of the interpretations offered by Stuke (46) is now known as the Burstein effect. The large Burstein effect in CdO is caused by a high curvature of the conduction band so that the effective mass should be small. Indeed, a value of 0.14 at the bottom of the conduction band has been found, which is exceptionally small for an oxide semiconductor. The dependence of the effective mass on carrier concentration points to a considerable deviation from the square dependence of energy on wave vector at higher energy states (50) so that the conduction band must be nonparabolic.

The low effective electron mass indicates potentially high mobilities. In single crystals and sintered polycrystals approximately 300 cm^2 V^{-1} sec^{-1} was measured for 10^{19} cm^{-3} electrons (50, 52). The highest value achieved in films (54) is 120 cm^2 V^{-1} sec^{-1} at almost 10^{20} cm^{-3} free electrons. Thin-film mobility data reported by different authors vary considerably. The causes for these variations may be found

in different film crystallization (54), grain boundaries (47), and impurities (44). Evidence has also accumulated for the occurrence of metallic cadmium as a separate phase in CdO films (46) and powders (55). The nature of this secondary phase affects not only the electrical parameters of a CdO film but its optical transmission as well.

The transparent electrode performance of CdO was studied in selenium photovoltaic cells (56) and silicon photodiodes (57). Transmission values between 80–90% were obtained at wavelengths longer than 5000 Å in samples with 220 ohm/sq sheet resistance. These properties should be subject to improvement since the electrical conductivities of the films in question were low (10^2 ohm^{-1} cm^{-1}). The highest reported conductivity of thin film CdO is 2000 ohm^{-1} cm^{-1} (44), which has been surpassed only by two other oxides of high transparency—Cd_2SnO_4 and In_2O_3.

Two particular characteristics are responsible for CdO not receiving more attention for practical utilization. Its transmission cut-off in the high-conductivity state (2.7 eV) leads to absorption of blue light so that the films appear green. More serious is a low resistance against atmospheric moisture attack (58), which excludes CdO films from many applications.

Tin Oxide

Tin oxide (SnO_2) has been the first and, until recently, the only transparent conductor which enjoyed significant commercialization. A combination of circumstances has favored this situation. First of all, tin oxide has acceptable electrical and optical properties. Of equal importance are its excellent chemical stability and mechanical hardness. Furthermore, simple and inexpensive fabrication methods based on low-cost raw materials became available early. Although these techniques did not yield a product with maximum possible conductivity and transmission, for many years a large demand for better coatings did not exist.

The technical importance of transparent tin oxide conductors has instigated research and development work which resulted in numerous publications and patents. A critical analysis of this vast body of literature frequently uncovers inconsistencies and contradictions. It is not intended here to present a comprehensive review of the existing literature on SnO_2, but rather to evaluate those properties pertinent to the utilization of SnO_2 as transparent conducting coating.

The intrinsic electrical and optical properties of SnO_2 could be elucidated in some detail after methods for the growth of high-quality single crystals were developed (59, 60). In fact, crystals were grown suitable for an accurate determination of the effective-mass tensor by submillimeter cyclotron resonance (61). These measurements yielded a density-of-states effective mass of 0.275 m_0 and the tensor components $m_\perp = 0.299\ m_0$ and $m_\parallel = 0.234\ m_0$ which are defined in reference to the c-axis of the tetragonal SnO_2 crystal structure (rutile).

High-quality SnO_2 crystals were also used for a detailed investigation of the electrical transport mechanism. The effects of different lattice-scattering modes could be separated from impurity and defect scattering (62). In high-purity crystals ($n \sim 10^{15}$ cm^{-3}) polar optical mode scattering was found to dominate above 250 K while below this temperature acoustic deformation potential scattering determines

the electron mobility until impurity and defect scattering prevail. The controlling influence of ionized impurity scattering shifts to higher temperatures with increasing doping and dominates at room temperature in crystals with $n > 10^{19}$ cm^{-3}.

Tin oxide is an *n*-type semiconductor. The native defects in high-purity crystals have been identified as doubly ionized oxygen vacancies with ionization energies of 30 meV and 150 meV (63). Their concentration can be varied over a wide range by heat treatment (64, 65). Antimony is another convenient donor (66), while in certain thin films prepared by hydrolysis, chlorine may provide free electrons (67).

The availability of high-purity SnO_2 single crystals has also made reliable optical measurements possible. The tetragonal crystal symmetry induces a large dichroism, and direct energy gap values of 3.57 eV and 3.93 eV were found for light polarized perpendicular and parallel to the *c*-axis, respectively (68). These values agree quite well with data derived from calculations of the energy band structure (69). In the near-infrared part of the spectrum free-carrier absorption occurs and appears to be caused by polar optical mode scattering (70), in agreement with the results of the electrical transport measurements.

The single-crystal data show that thin films of SnO_2 should have useful transparent electrode properties. The size of the band gap assures that light will be transmitted over the whole visible spectrum, and the reported mobility values (62) should lead to acceptable conductivities. Work with SnO_2 thin films (71) started long before the single-crystal investigations, and their potential for transparent conductor applications was soon recognized (8, 72, 73). The quality of the coatings depends very much on the method of deposition. Many different techniques have been described in the literature, including vacuum evaporation of tin metal and subsequent oxidation (71, 74), reactive RF sputtering of tin (58), sputtering from oxide cathodes (75), spray deposition of tin-salt solutions (66, 76), chemical vapor deposition (77, 78), and *d-c* glow discharge (79). The quoted references are by no means exhaustive and many more can be found in the literature cited as well as in a recent summary (80).

The results of the thin-film investigations are subject to a meaningful interpretation only if the samples have been fully characterized and their structure and composition are known. Thin films can consist of more than one phase if this is thermodynamically favored. In the case of tin oxide it has not always been recognized that tin and oxygen form SnO_2 as well as SnO, Sn_2O_3 (81), and possibly other phases. Depending on the deposition conditions any one of these phases may form. Direct evidence for the presence of SnO in vapor-deposited SnO_2 films has been reported (67). In other vapor-deposited Sb-doped films, Sb_2O_4 and additional unidentified phases were detected (77). A detailed analysis of the SnO_2 deposition by reactive sputtering has shown that the presence of SnO depends on a number of experimental parameters (82). The film composition was found to be influenced by the plasma pressure and composition, the discharge voltage, and the target-substrate distance.

It is not difficult to see that secondary phases may alter the electrical and optical properties of a SnO_2 film. Considering SnO, the most likely secondary phase, a reduction of the optical film transmission is to be expected. Depending on the particular modification, powders of SnO are either blue-black or red, indicating a small band gap. Data on SnO thin films also show a lower optical transmission

than for SnO_2 films (83). The effect of SnO on the electrical properties of SnO_2 films is more difficult to predict in the absence of experimental information, but it is unlikely that the electrical conductivity remains unaffected.

Summarizing the information, which was most likely obtained on single-phase SnO_2 films, the following picture emerges. The absorption edge of thin SnO_2 films is located at approximately 3.7 eV. Its position depends on the free-electron concentration, and a small Burstein shift of about 0.1 eV has been observed (83, 84). Electron mobilities at 300 K are low, in general of the order of 10 cm^2/V-sec. The highest reported electrical conductivities are in the 1200–1400 ohm^{-1} cm^{-1} range (76, 85) and may be subject to improvement if higher mobilities can be achieved.

The transparent conductor properties of commercial tin oxide coatings have stagnated for many years with sheet resistances in the 100–200 ohm/sq range and visible transmission values of 80–85%. Most of these films were doped with antimony, and their transmission decreases appreciably if sheet resistances of less than 100 ohm/sq are desired (86). Notable advances have been made recently (87). Figure 3 shows the optical transmission spectrum of a 12 ohm/sq tin oxide film on soda lime glass. The sample was obtained through the courtesy of J. F. Jordan, Photon Power, Inc. Interestingly, this coating was prepared by a simple spray-deposition technique, which in general is not considered to yield outstanding transparent electrodes. The inexpensive soda lime substrate might be suspected to lead to severe film contamination by alkali ions and other impurities during the deposition process.

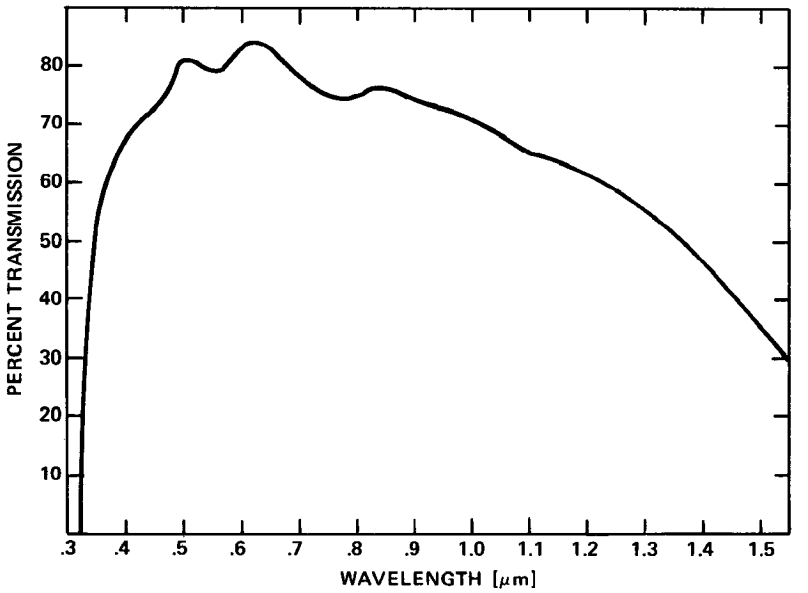

Figure 3 Optical transmission of 12 ohm/sq tin oxide film coated onto soda lime substrate by spray deposition.

The electrical and optical film properties, however, do not appear to have suffered significantly from whatever impurities diffused into the sample.

Indium Oxide

Commercial utilization of indium oxide (In_2O_3) coatings began only a few years ago, even though the transparent electrode properties of In_2O_3 have been known for quite some time. Much of the impetus for substituting SnO_2 by In_2O_3 came from the need for transparent electrodes in liquid-crystal displays. Here, close tolerances of the flatness of the electrodes are essential, and can best be achieved by the low-temperature vacuum-deposition processes (sputtering, evaporation) developed for indium oxide. Equally important is the fact that In_2O_3 can be etched more easily than tin oxide. This behavior facilitates a more economical photo-etching procedure during the manufacture of digital displays. Although chemically less inert than SnO_2, the stability of indium oxide is adequate for many applications.

The fundamental materials parameters of In_2O_3 are not as well known as for SnO_2. Indium oxide single crystals of a quality comparable to the best SnO_2 crystals have not yet been prepared. While SnO_2 crystals with room-temperature electron concentrations of 7×10^{15} cm^{-3} have been reported (61), the lowest free-electron concentration achieved in In_2O_3 crystals is still higher than 10^{17} cm^{-3} (88). A consequence of this situation is our lack of knowledge of reliable effective mass values. Effective masses quoted in the literature range from 0.2–0.5 m_0 (88–91). Published mobility data favor an effective mass closer to the lower end of the quoted range.

Optical measurements on In_2O_3 single crystals (92) have identified the onset of direct transitions at 3.75 eV. A weak absorption starting at 2.6 eV is probably caused by indirect transitions. Thin-film investigations arrived at an energy gap of 3.65 eV (93). Magnetoresistance measurements provided some additional information on the band structure (94). The constant energy surfaces in the conduction band were found to consist either of warped spheres or ellipsoids along the [111] and [110] axes.

Electrical transport studies on In_2O_3 crystals led to the conclusion that the charge carriers are scattered by acoustical lattice modes and by ionized impurities (88). At temperatures above 1100°C the carrier transport is determined by compound decomposition (95). The native defects causing *n*-type conduction in undoped specimens may be interstitial indium ions (96).

The conduction mechanism in thin films is more complicated than in single crystals and is strongly influenced by the deposition technique. In some films prepared by reactive sputtering, highly resistive depletion layers at the grain boundaries are believed to control the mobility at low-carrier concentrations while, with increasing degeneracy, bulk effects repress the grain-boundary influence (93). Interesting observations were made on spray-coated samples containing different dopants (97). Films sprayed from solutions with no dopant added intentionally had mobilities between 55 and 60 cm^2/V-sec and approximately 10^{19} cm^{-3} free electrons. Doping with tin generated more electrons and the mobility increased to 75 cm^2/V-sec when the electron concentration reached 10^{20} cm^{-3}. Even higher mobilities resulted from titanium doping (120 cm^2/V-sec, 10^{20} cm^{-3} electrons). The

highest mobility (170 cm^2/V-sec) was achieved in zirconium-doped specimens having 8×10^{19} cm^{-3} electrons. Such values, at the reported carrier concentrations, are uncommonly high for thin-film semiconductors, and it is unfortunate that these observations have not been followed up by other investigators. The dominating scattering mechanism in the above coatings was assumed to be grain-boundary scattering.

Groth (97) also provided information on the transparent conductor properties of In_2O_2 films. Best results were achieved with tin doping. Since then tin has become the standard dopant in transparent indium oxide conductors, and a number of papers published in recent years discuss the properties of these films prepared by sputter deposition (91, 98–101). Rather detailed investigations of the dependence of film behavior on a host of sputtering parameters are presented in these publications. This information is not repeated here since the results obtained in sputtering systems of different design do not always agree.

The transparent electrode properties disclosed in the preceding references represent the state-of-the-art technology of sputter-coated tin-doped In_2O_3. Salient features of these coatings are as follows. The highest reported electrical conductivity is 5600 ohm^{-1} cm^{-1} (99). Electron mobilities of approximately 40 cm^2/V-sec at 7×10^{20} cm^{-3} free carriers have been observed (91). The index of refraction at 5500 Å can be as low as 2.0, but values approaching 2.5 were measured in films subjected to specific heat treatments (101). The lowest sheet resistance recorded is 1.6 ohm/sq, which was obtained in a film with 73% optical transmission at 5000 Å wavelength (99). Films with 2–3 ohm/sq sheet resistance were estimated to transmit 95% of the visible light when reflection losses caused by the high index of refraction could be eliminated (101).

Figure 4 shows optical transmission characteristics of Sn : In_2O_3 films representing the current state of development. Comparing this figure with Figure 3 proves that the electrical and optical properties of indium oxide films exceed those of tin oxide. The high transparency of the spray-coated film in Figure 4 is rather surprising. As a matter of fact, this film has a larger figure of merit ϕ_{TC} (3.1×10^{-2} ohm^{-1}) at 5500 Å than the 7.2 ohm/sq film prepared by sputter coating ($\phi_{TC} = 2.4 \times 10^{-2}$ ohm^{-1}). Still higher ϕ_{TC}'s, however, have been achieved in sputtered films. From data reported by Fraser & Cook (99) ($T = 0.83$, $R_s = 3.1$ ohm/sq) a figure of merit of 5.2×10^{-2} ohm^{-1} can be calculated.

Several papers provide information on the utilization of In_2O_3 electrodes in combination with photoconductors for use in optically addressable light valves, photodetectors, or storage devices. Older publications discuss the preparation and properties of transparent In_2O_3 contacts on single crystals of CdS (102) and ZnS (103). Recently, In_2O_3 electrodes were prepared together with CdS (104) and $Cd_{1-x}Zn_xS$ films (105), and the optical and electrical properties of the composite layer structures investigated.

Cadmium Stannates

The CdO/SnO_2 phase diagram contains two distinct chemical compounds: Cd_2SnO_4 and $CdSnO_3$ (106, 107). Both compounds normally crystallize in the ortho-

rhombic structure, and they are *n*-type wide-band-gap semiconductors. Current knowledge of their intrinsic semiconducting properties is fragmentary. The fundamental parameters, such as band gap and effective mass, have not yet been well established, but sufficient information demonstrating the utility of these materials as transparent conducting coatings is available. It also indicates that basic studies of the cadmium stannates may provide valuable scientific data. This is particularly

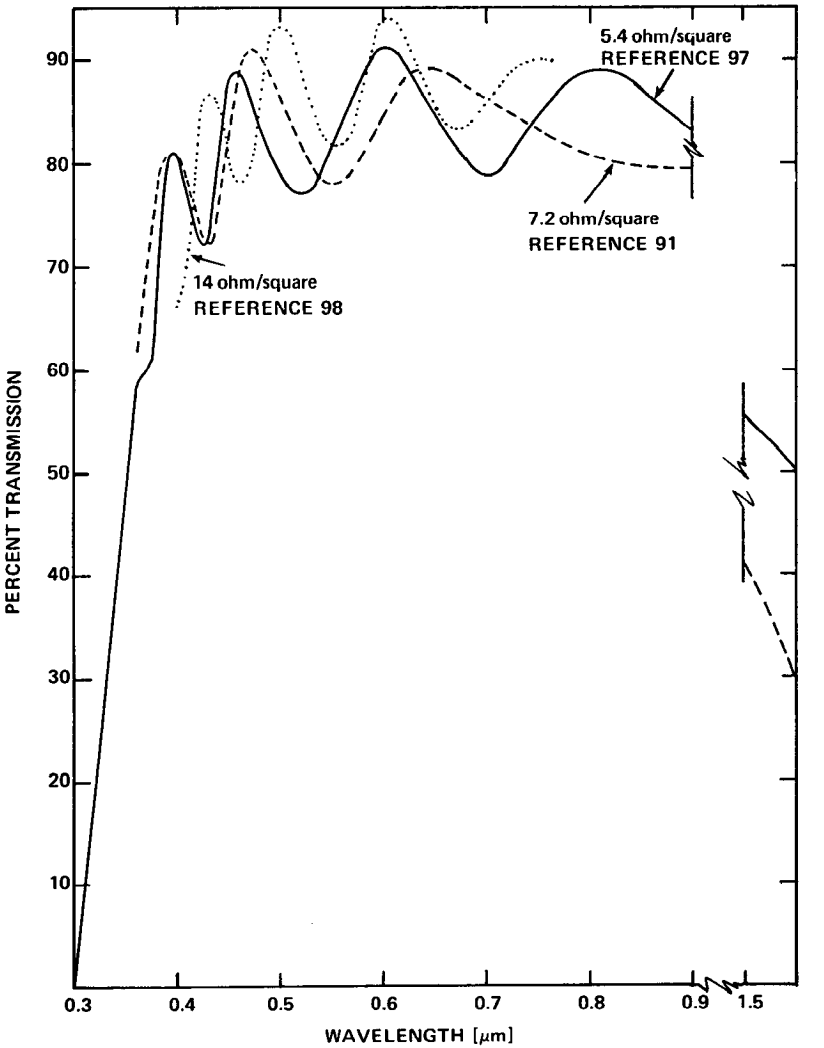

Figure 4 Transmission spectra of Sn : In_2O_3 films; 5.4 ohm/sq film is spray coated, 7.2 ohm/sq and 14 ohm/sq films are sputter coated.

true for thin-film investigations where the stannates could serve as model systems for clarifying the role of multiphase composition on electrical conduction and optical transparency.

Prior to 1972 the cadmium stannates were largely unknown. Metastannate was mentioned to be a semiconductor, but additional information was not provided (108). It crystallizes in a hexagonal form (ilmenite) when coprecipitated from solution and subsequently fired at 900°C (109). Heat treatment at 1000°C converts the ilmenite phase to the orthorhombic structure. Even less has been reported on Cd_2SnO_4; only structural data and a description of its bright yellow color became a matter of public record (110).

The first information on the semiconducting properties of Cd_2SnO_4 emerged from measurements on powder samples and thin amorphous films prepared by RF sputtering (111). The color of the powder samples was found to depend on the preparation conditions. When synthesized in an oxidizing atmosphere the powders are bright yellow. Deep green samples result when a reducing environment exists during synthesis. Diffuse reflection spectra show a displacement of the optical absorption edge from 2.34 eV to 2.76 eV. The absorption-edge shift is accompanied by an increase of the powder conductivity over several orders of magnitude.

An even more impressive shift of the absorption edge takes place in sputter-coated Cd_2SnO_4 films when the RF plasma is changed from an oxidizing composition to a highly reducing atmosphere or when the samples are subjected to a post-deposition heat treatment. In amorphous films, the absorption edge moves from 2.06 eV to 2.85 eV, turning the color of the films from brown to light green (111). Simultaneously with the color change the carrier density increases from 10^{17} to 10^{20} cm^{-3}. It is suggestive to interpret these observations as Burstein effects. The effective electron mass following from such an interpretation would be 0.04 m_0, which is inexplicably low for a wide-band-gap oxide semiconductor.

Clarifying information on the optical effects came from studies of polycrystalline Cd_2SnO_4 films (16). These films, when prepared by RF sputtering, do not crystallize in the orthorhombic structure but produce a cubic X-ray diffraction spectrum (L. A. Siegel, private communication). Careful analysis of the X-ray spectra reveals that the sputtered crystalline Cd_2SnO_4 films are not single-phase but contain CdO and sometimes $CdSnO_3$. The deposition conditions can be adjusted to avoid the $CdSnO_3$ phase. However, CdO has always been observed unless a negative bias voltage is applied to the substrate. Then, the CdO phase diminishes with increasing bias and at approximately -200 volts the X-ray spectrum is free of CdO lines. Unfortunately, these films are still not single-phase since at higher bias voltages the presence of $CdSnO_3$ is evident.

The crystalline films, like amorphous specimens, are brownish when sputtered in pure oxygen. Annealing in argon shifts the absorption edge to shorter wavelengths by approximately the same amount found in amorphous coatings. The CdO phase is still present after the argon annealing. It disappears only when the samples are exposed to temperatures higher than 700°C, in which case the electrical resistance rapidly approaches insulator values.

A second technique of eliminating the CdO phase from sputtered Cd_2SnO_4 films

utilizes a CdS/Ar atmosphere during the post-deposition annealing (112). Under these conditions, the film conductivity is not lost but, on the contrary, increases considerably. While optimal annealing in argon leads to approximately 3000 ohm^{-1} cm^{-1}, conductivity values as high as 6500 ohm^{-1} cm^{-1} have been measured after CdS/Ar treatment. The optical transmission characteristics also improve if CdS/Ar is substituted for argon in the heat-treatment step.

The results obtained in crystalline Cd_2SnO_4 films suggest that the large absorption-edge shift is not exclusively caused by an intrinsic property of Cd_2SnO_4. Instead, the well-established Burstein effect of CdO (46, 48) is likely to be a major contributor. The Burstein effect cannot be ruled out in Cd_2SnO_4 in view of the observations made on powder samples (111). But the total edge shift in sputtered films appears to be composed of the effects present in both CdO and Cd_2SnO_4. The limited information currently available does not allow one to separate the individual contributions of the two materials.

The value of the energy gap in Cd_2SnO_4 films is doubtful if we accept the validity of the preceding arguments; it should be larger than 2.06 eV. But since low-conductivity single-phase films have not yet been prepared, reliable measurements are still missing. The smallest gap found from diffuse reflectance measure-

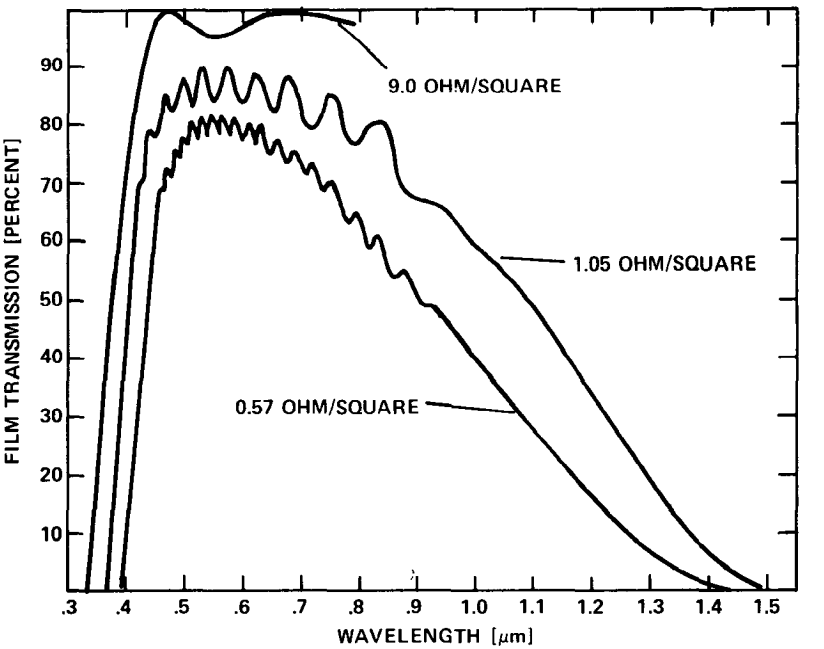

Figure 5 Transmission spectra of sputter-coated Cd_2SnO_4 films deposited onto different substrate materials; 9.0 ohm/sq film on single-crystal sapphire, 1.05 ohm/sq film on silica, 0.57 ohm/sq film on Corning 1720.

ments in Cd_2SnO_4 powders is 2.34 eV. This is not necessarily the correct gap for thin films since they have a different crystal structure.

Despite our limited knowledge of the basic materials parameters of Cd_2SnO_4 its excellent transparent conductor properties have been firmly established (16, 19). Coatings can be prepared routinely by RF sputtering which have approximately 1 ohm/sq sheet resistance and 85% average transmission at 5500 Å. Examples of the optical transmission spectra of such films with different sheet resistances are shown in Figure 5 (see also 16). Substrate absorption has been eliminated from these curves so that different films can be compared on the basis of their intrinsic properties alone. A figure of merit $\phi_{TC} = 21.1 \times 10^{-2}$ ohm^{-1} at 5500 Å wavelength is calculated for the 1.05 ohm/sq film using an average transmission value of 0.86.

Very thin coatings of Cd_2SnO_4 ($1–2 \times 10^{-5}$ cm) have high luminous transmittances. Films on Corning 7059 glass with 15 ohm/sq sheet resistance were found to have 86–87% total luminous transmittance (substrate absorption included). The preparation of these coatings requires only 7 min deposition time under optimized sputter conditions.

The substrate material can influence the film properties considerably. One example is included in Figure 5. The 9 ohm/sq coating was deposited onto a single-crystal sapphire substrate. Its high transmission is remarkable because this film was heat treated in argon only, and therefore has a low conductivity (3200 ohm^{-1} cm^{-1}). Corning 7059 glass is a most suitable substrate. Good results were also achieved

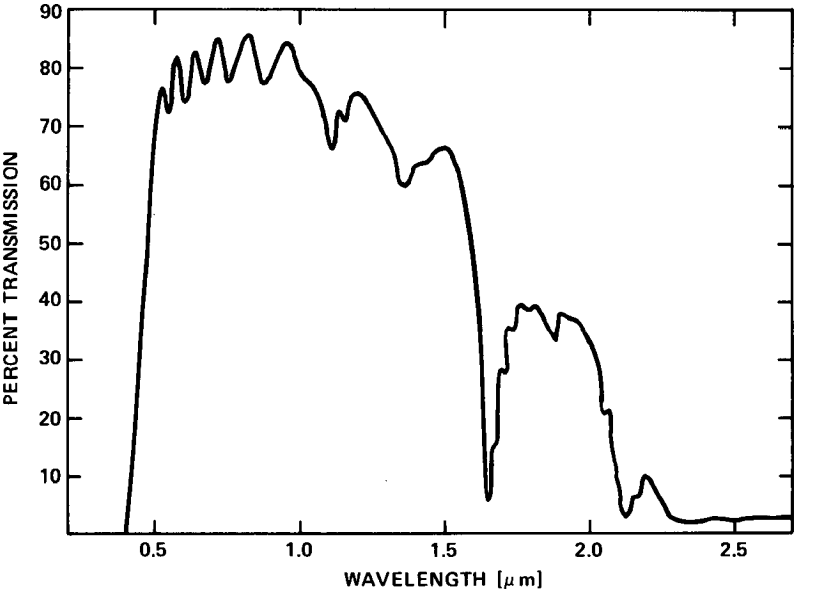

Figure 6 Optical transmission of Cd_2SnO_4 film sputter-coated onto Lexan substrate; sheet resistance is 8 ohm/sq.

with Corning 1720 alumino silicate which, however, is difficult to obtain. Silica glass offers convenience but a large mismatch of its coefficient of thermal expansion with that of Cd_2SnO_4 induces film cracking in very low sheet-resistance samples ($R_s < 1$ ohm/sq).

Transparent conductive Cd_2SnO_4 coatings can also be sputtered onto plastic substrates. The low temperature stability of these organic materials requires preparation conditions leading to amorphous films. Their transparent conductor properties are inferior to polycrystalline coatings. This can be inferred from Figure 6, which shows the transmission spectrum of a Cd_2SnO_4 film on a polycarbonate substrate. The 8 ohm/sq sheet resistance is still competitive with commercial gold films on plastics.

The potential of transparent cadmium stannate conductors for large-area applications has prompted the investigation of deposition methods other than RF sputtering. Spray deposition of Cd/Sn-containing solutions onto hot substrates has given encouraging results (113). In this preparation technique the substrate temperature determines the film composition. At high temperatures ($\gtrsim 800°C$) the Cd_2SnO_4 phase forms, while at lower temperatures ($\lesssim 700°C$) the coatings consist of $CdSnO_3$. Both phases are present in specimens prepared in the intermediate temperature range.

In view of the experimental difficulties associated with high-temperature spray deposition, attempts to prepare the Cd_2SnO_4 phase have been limited to exploratory experiments. Clear films with approximately 100 ohm/sq sheet resistance were obtained on silica substrates. These samples did not contain CdO, but the X-ray spectra indicated varying concentrations of $CdSnO_3$.

Lower sheet resistances were achieved in coatings containing the $CdSnO_3$ phase only. Films with sheet resistances in the 10–15 ohm/sq range can be spray-deposited within 3–4 min and do not require a post-deposition heat treatment. Their optical transmission is between 75–85% in the 5500–7500 Å wavelength range. Coatings with 5–10 ohm/sq have also been prepared, but their transmission characteristics need to be improved.

Projecting further improvements of spray-coating technology, it appears reasonable that higher optical transmissions will become feasible in $CdSnO_3$ films with 10–15 ohm/sq as well as lower sheet resistances. The experimental data are not sufficient to predict whether the high quality of low sheet-resistance sputtered Cd_2SnO_4 coatings can be duplicated in sprayed films. Other deposition techniques, such as reactive sputtering or chemical vapor deposition, have not yet been assessed and may yield interesting results.

Cadmium stannate coated onto glass substrates is highly resistant to abrasion and adheres extremely well. The layers can be removed only with a diamond stylus or by an acid etch. Patterns have been successfully etched into low-resistance films by photo-etching. In this respect cadmium stannate resembles indium oxide.

The adherence of sputtered cadmium stannate onto plastics is generally inadequate, but this deficiency can be ameliorated through deposition of thin oxide interlayers, which also improve the abrasion resistance.

The general environmental stability of Cd_2SnO_4 is good. No changes in conductivity or transmission have been detected after many months of shelf storage. Normal

atmospheric humidity does not appear to impair the film properties, and low-temperature cycling tests at 95% relative humidity (MIL-STD-810) did not induce visible deterioration of the test samples.

CONCLUSIONS

The last decade has seen impressive advances in the development of transparent conducting coatings. Progress came not only from improved performance characteristics of proven materials but from new compounds added to the list from which candidates can be chosen for a particular application. Besides gold, three semiconductors are available.

The required sheet resistance is normally a starting point for selecting a suitable transparent conductor. If resistance values near 100 ohm/sq or higher are specified, any one of the three oxides—tin oxide, indium oxide, or cadmium stannate—qualifies since the transmission differences are small in this resistance range. Cost advantages, etching behavior, and others will then determine the right choice.

Sheet resistances in the 10–20 ohm/sq region are currently most easily accessible with In_2O_3 or Cd_2SnO_4. Tin oxide coatings absorb more light than the other two oxides and could only be used if the optical requirements are relaxed.

When a coating with 1–10 ohm/sq sheet resistance is needed the selection has to be made between Cd_2SnO_4 and In_2O_3. Tin oxide films with competitive transmission characteristics have not yet been reported. A clear choice between Cd_2SnO_4 and In_2O_3 based on their electrical and optical properties alone is difficult to make. Published data indicate that near 1 ohm/sq the optical absorption of Cd_2SnO_4 is lower beyond 5000 Å wavelength while, in the short wavelength range, In_2O_3 transmits more efficiently due to its larger energy gap.

Chemical stability, etching behavior, hardness, and abrasion resistances are quite similar in In_2O_3 and Cd_2SnO_4. The heat treatment required for sputtered cadmium stannate films could present a cost disadvantage. However, this treatment is specific for sputtered films and may not be needed when the coatings are prepared by other fabrication processes. Spray deposition, for example, is a fast technique which does not require post-deposition annealing.

Raw materials considerations would play a role when large scale applications are contemplated. The question of indium availability is still controversial. According to one estimate (114) the total world indium reserves would be insufficient to consider indium compounds for the anticipated volume of solar energy converters. Proponents of indium-containing devices argue that the earth's crust contains enormous amounts of indium. But it remains to be shown how much of this could be mined economically. The price differential between indium and cadmium/tin is another factor that may favor cadmium stannate if cost is critical.

In venturing a prediction of future development it appears likely that still better transparent conducting coatings will be developed. Neither indium oxide nor cadmium stannate seems to have reached its full potential. And the example of cadmium stannate shows that there is always a chance of new material being discovered.

Literature Cited

1. Bidwell, C. 1885. *Philos. Mag.* 20:178–91
2. Von Uljanin, W. 1888. *Ann. Phys. Leipzig* 34:241–73
3. Fritts, C. E. 1884. *Proc. Am. Assoc. Adv. Sci.* 33:97–108
4. Lange, B. 1930. *Phys. Z.* 31:964–69
5. Bergmann, L. 1931. *Phys. Z.* 32:286–88
6. Duhme, E., Schottky, W. 1930. *Naturwissenschaften* 18:735–36
7. Teichmann, H. 1931. *Z. Phys.* 67:192–93
8. *Br. Patent* 632,256. 1942.
9. *US Patent* 2,516,663. 1950.
10. Gillery, F. H. 1972. *Inf. Disp.* 9:17–19
11. Heilmeier, G. H., Zanoni, L. A., Barton, L. A. 1968. *Appl. Phys. Lett.* 13:46–47
12. Giglia, R. D. 1975. *Int. Symp. Soc. Inf. Disp. Wash. DC*, pp. 52–53
13. Jordan, J. F. 1973. *Proc. Photovolt. Conv. Solar Energy Terrest. Appl. Vol. II, Cherry Hill, NJ*, pp. 182–86
14. Haacke, G. 1973. See Reference 13, p. 289
15. Burton, L. C., Hench, T., Storti, G., Haacke, G. 1976. *J. Electrochem. Soc.* 123:1741–44
16. Haacke, G. 1976. *Appl. Phys. Lett.* 28: 622–23
17. Fan, J. C. C., Reed, T. B., Goodenough, J. B. 1974. *Proc. 9th Intersoc. Energy Conv. Eng. Conf., San Francisco*, pp. 341–46
18. Haacke, G. 1977. *Appl. Phys. Lett.* In press
19. Haacke, G. 1976. *J. Appl. Phys.* 47:4086–89
20. Fan, H. Y., Spitzer, W., Collins, R. J. 1956. *Phys. Rev.* 101:566–72
21. Dumke, W. P. 1961. *Phys. Rev.* 124: 1813–17
22. Jones, H. 1956. In *Handbuch der Physik*, ed. S. Flügge, 19:238. Berlin: Springer
23. Pearson, G. L., Bardeen, J. 1949. *Phys. Rev.* 75:865–83
24. Chopra, K. L., Bobb, L. C., Francombe, M. H. 1963. *J. Appl. Phys.* 34:1699–1702
25. Keyes, R. W. 1959. *J. Appl. Phys.* 30: 454
26. Sennett, R. S., Scott, G. D. 1950. *J. Opt. Soc. Am.* 40:203–11
27. Nossek, R. 1955. *Z. Phys.* 142:321–33
28. Chopra, K. L. 1969. *Thin Film Phenomena*. New York: McGraw-Hill. 844 pp.
29. Cornely, R. H., Fuschillo, N. 1974. *J. Vac. Sci. Technol.* 11:163–66
30. Stirn, R. J., Yeh, Y. C. M. 1975. *Appl. Phys. Lett.* 27:95–98
31. Gillham, E. J., Preston, J. S. 1952. *Proc. Phys. Soc. London Sect. B* 65:649
32. Gillham, E. J., Preston, J. S., Williams, B. E. 1955. *Philos. Mag.* 46:1051–68
33. Ennos, A. E. 1957. *Br. J. Appl. Phys.* 8:113–17
34. Schneider, M. V. 1966. *Bell Syst. Tech. J.* 45:1611–38
35. Reynolds, F. W., Stilwell, G. R. 1952. *Phys. Rev.* 88:418–19
36. Anderson, W. A., Delahoy, A. E. 1972. *Proc. IEEE* 60:1457–58
37. Anderson, W. A., Delahoy, A. E., Milano, R. A. 1973. See Reference 13, pp. 209–18
38. Fuschillo, N., Lalevic, B., Slusark, W., Delahoy, A. 1975. *J. Vac. Sci. Technol.* 12:84–87
39. Hoffman, D. M., Coutts, M. D. 1976. *J. Vac. Sci. Technol.* 13:122–26
40. Cox, R. E. L., Hersee, S. D. 1972. *Thin Solid Films* 11:323–28
41. Hrostowski, H. J., Wheatley, G. H., Flood, W. F. 1954. *Phys. Rev.* 95:1683–84
42. Hilsum, C., Rose-Innes, A. C. 1961. *Semiconducting III-V Compounds*, p. 128. New York: Pergamon. 239 pp.
43. Anderson, J. C. 1970. *Adv. Phys.* 19:311–38
44. Helwig, G. 1952. *Z. Phys.* 132:621–42
45. Lappe, F. 1954. *Z. Phys.* 137:380–82
46. Stuke, J. 1954. *Z. Phys.* 137:401–15
47. Finkenrath, H. 1960. *Z. Phys.* 158:511–32
48. Finkenrath, H. 1960. *Z. Phys.* 159:112–24
49. Miloslavskii, V. K., Ranyuk, A. I. 1961. *Opt. Spectrosc.* 11:289–92
50. Finkenrath, H., von Ortenberg, M. 1967. *Z. Angew. Phys.* 23:323–28
51. Koffyberg, F. P. 1970. *J. Solid State Chem.* 2:176–81
52. Koffyberg, F. P. 1971. *Can. J. Phys.* 49: 435–40
53. Burstein, E. 1954. *Phys. Rev.* 93:632–33
54. Tanaka, K., Kunioka, A., Sakai, Y. 1969. *Jpn. J. Appl. Phys.* 8:681–91
55. Straumanis, M. E., Vora, P. M., Khan, A. A. 1971. *Z. Anorg. Allgem. Chem.* 383:211–19
56. Preston, J. S. 1950. *Proc. R. S. London Ser. A* 202:449–66
57. Kondo, R., Okimura, H., Sakai, Y. 1971. *Jpn. J. Appl. Phys.* 10:1547–54
58. Holland, L., Siddall, G. 1953. *Vacuum* 3:375–91
59. Marley, J. A., MacAvoy, T. C. 1961. *J. Appl. Phys.* 32:2504–5
60. Fonstad, C. G., Linz, A., Rediker, R. H. 1969. *J. Electrochem. Soc.* 116:1269–71
61. Button, K. J., Fonstad, C. G., Dreybrodt, W. 1971. *Phys. Rev. Sect. B* 4:4539–42

62. Fonstad, C. G., Rediker, R. H. 1971. *J. Appl. Phys.* 42:2911–18
63. Samson, S., Fonstad, C. G. 1973. *J. Appl. Phys.* 44:4618–21
64. Marley, J. A., Dockerty, R. C. 1965. *Phys. Rev. Sect. A* 140:304–10
65. Nagasawa, M., Shionoya, S. 1971. *Jpn. J. Appl. Phys.* 10:727–31
66. Aitchison, R. E. 1954. *Aust. J. Appl. Sci.* 5:10–17
67. Aboaf, J. A., Marcotte, V. C., Chou, N. J. 1973. *J. Electrochem. Soc.* 120:701–2
68. Summitt, R., Marley, J. A., Borrelli, N. F. 1964. *J. Phys. Chem. Solids* 25:1465–69
69. Arlinghaus, F. J. 1974. *J. Phys. Chem. Solids* 35:931–35
70. Summitt, R., Borrelli, N. F. 1965. *J. Phys. Chem. Solids* 26:921–25
71. Bauer, G. 1937. *Ann. Phys. Leipzig* 30: 433–45
72. *US Patent* 2,429,420. 1947.
73. Ward, J. W. 1955. *Appl. Ind.* 16:408–16
74. Watanabe, H. 1970. *Jpn. J. Appl. Phys.* 9:1551
75. Vossen, J. L., Poliniak, E. S. 1972. *Thin Solid Films* 13:281–84
76. Fischer, A. 1954. *Z. Naturforsch. Teil A* 9:508–11
77. Kane, J., Schweizer, H. P., Kern, W. 1976. *J. Electrochem. Soc.* 123:270–77
78. Baliga, B. J., Ghandhi, S. K. 1976. *J. Electrochem. Soc.* 123:941–44
79. Carlson, D. E. 1975. *J. Electrochem. Soc.* 122:1334–37
80. Jarzebski, Z. M., Marton, J. P. 1976. *J. Electrochem. Soc.* 123:199C–205C
81. Murken, G., Trömel, M. 1973. *Z. Anorg. Allg. Chem.* 397:117–26
82. Hecq, M., Portier, E. 1972. *Thin Solid Films* 9:341–55
83. Arai, T. 1960. *J. Phys. Soc. Jpn.* 15:916–27
84. Spence, W. 1967. *J. Appl. Phys.* 38:3767–70
85. Redaelli, G. 1976. *Appl. Opt.* 15:1122–23
86. Peaker, A. R., Horsley, B. 1971. *Rev. Sci. Inst.* 42:1825–27
87. Jordan, J. F. 1974. *Second Natl. Sci. Found. Photovolt. Conv. Res. Prog. Rev. Philadelphia*, pp. 214–35
88. Weiher, R. L. 1962. *J. Appl. Phys.* 33: 2834–39
89. Vainshtein, V. M., Fistul, V. I. 1967. *Sov. Phys. Semicond.* 1:104–5
90. Müller, H. K. 1968. *Phys. Status Solidi* 27:733–40
91. Fan, J. C. C., Bachner, F. J. 1975. *J. Electrochem. Soc.* 122:1719–25
92. Weiher, R. L., Ley, R. P. 1966. *J. Appl. Phys.* 37:299–302
93. Müller, H. K. 1969. *Phys. Status Solidi* 27:723–31
94. Weiher, R. L., Dick, B. G. Jr. 1964. *J. Appl. Phys.* 35:3511–15
95. DeWit, J. H. W. 1975. *J. Solid State Chem.* 13:192–200
96. DeWit, J. H. W. 1973. *J. Solid State Chem.* 8:142–49
97. Groth, R. 1966. *Phys. Status Solidi* 14: 69–75
98. Vossen, J. L. 1971. *RCA Rev.* 32:289–96
99. Fraser, D. B., Cook, H. D. 1972. *J. Electrochem. Soc.* 119:1368–74
100. Pankratz, J. M. 1972. *J. Electron. Mater.* 1:182–90
101. Molzen, W. W. 1975. *J. Vac. Sci. Technol.* 12:99–102
102. Sihvonen, Y. T., Boyd, D. R. 1960. *Rev. Sci. Instrum.* 31:992–94
103. Williams, V. A. 1966. *J. Electrochem. Soc.* 113:234–37
104. Mehta, R. R., Vogel, S. F. 1972. *J. Electrochem. Soc.* 119:752–56
105. Fraser, D. B. 1972. *Thin Solid Films* 13:407–12
106. Smith, A. J. 1960. *Acta Crystallogr.* 13: 749–52
107. Trömel, M. 1969. *Z. Anorg. Allgem. Chem.* 371:237–47
108. Coffeen, W. W. 1953. *J. Am. Ceram. Soc.* 36:207–14
109. Morgenstern-Badarau, I., Poix, P., Michel, A. 1963. *Comp. Rend.* 256:692–93
110. Hassanein, M. 1966. *J. Chem. UAR* 9:275–80
111. Nozik, A. J. 1972. *Phys. Rev. Ser. B* 6:453–59
112. Haacke, G. 1976. *Proc. 2nd ERDA Semiann. Solar Photovolt. Conv. Progr. Conf. Lake Buena Vista*, pp. 683–98
113. Haacke, G. 1975. *Proc. 1st ERDA Semiann. Solar Photovolt. Conv. Progr. Conf. Los Angeles*, pp. 661–76
114. Executive Report, October 1974. *Conf. Photovolt. Conv. Solar Energy Terrest. Appl. Cherry Hill, NJ*, p. 5

CONTENTS

PREFATORY CHAPTER

POINT DEFECTS AND THEIR INTERACTION, *Carl Wagner* 1

STRUCTURE

DEFECT CHEMISTRY IN CRYSTALLINE SOLIDS, *F. A. Kröger* 449

DEEP LEVEL IMPURITIES IN SEMICONDUCTORS, *H. G. Grimmeiss* 341

STRUCTURAL ASPECTS OF ONE-DIMENSIONAL CONDUCTORS, *Galen D. Stucky, Arthur J. Schultz, and Jack M. Williams* 301

PREPARATION, PROCESSING, AND STRUCTURAL CHANGES

STRUCTURAL TRANSFORMATIONS DURING AGING OF METAL ALLOYS, *Yu. D. Tiapkin* 209

HIGH RATE THICK FILM GROWTH, *John A. Thornton* 239

METAL FORMING: THE APPLICATION OF LIMIT ANALYSIS, *Betzalel Avitzur* 261

PROPERTIES AND PHENOMENA

KINETICS AND MECHANISMS OF GAS–METAL INTERACTIONS, *H. J. Grabke and G. Hörz* 155

EROSION, *Carolyn M. Preece and Norman H. Macmillan* 95

REVERSIBLE TEMPER EMBRITTLEMENT, *D. F. Stein* 123

ACOUSTIC EMISSION IN BRITTLE MATERIALS, *A. G. Evans and M. Linzer* 179

CAPACITANCE TRANSIENT SPECTROSCOPY, *G. L. Miller, D. V. Lang, and L. C. Kimerling* 377

HOT CORROSION OF HIGH-TEMPERATURE ALLOYS, *John Stringer* 477

FUNDAMENTAL OPTICAL PHENOMENA IN INFRARED WINDOW MATERIALS, *Bernard Bendow* 23

SPECIAL MATERIALS

DENTAL AMALGAM, *Svein Espevik* 55

TRANSPARENT CONDUCTING COATINGS, *G. Haacke* 73

INDEXES

AUTHOR INDEX 511

SUBJECT INDEX 524

CUMULATIVE INDEX OF CONTRIBUTING AUTHORS, VOLUMES 2–6 534

CUMULATIVE INDEX OF CHAPTER TITLES, VOLUMES 2–6 535